Inorg. Chem. **2008**, *47*, 7745−7750

Hydration of Hydrogentungstate Anions at Different pH Conditions: A Car−Parrinello Molecular Dynamics Study

Antonio Rodríguez-Fortea,* Laia Vilà-Nadal, and Josep M. Poblet*

Departament de Química Física i Inorgànica, Universitat Rovira i Virgili, C/Marcel·lí Domingo s/n, 43007 Tarragona, Spain

Received April 29, 2008

Standard density functional theory calculations with a continuous model of solvation as well as Car−Parrinello molecular dynamics simulations with explicit solvent molecules are carried out to analyze the effect of the pH of the solution on the coordination sphere of the W^{VI} ion. Both methodologies agree in predicting an expansion of the coordination sphere of the W^{VI} ion upon a decrease in the pH. Continuous solvation models, however, are unable to predict as stable some structural isomers of a hydrated hydrogentungstate anion and tungstic acid.

Introduction

Polyoxometalates (POMs) are an important class of polynuclear metal−oxygen cluster anions usually formed by W, Mo, or V and mixtures of these elements in their highest oxidation states. POMs feature unique structural and electronic characteristics that make them attractive for applications in many fields such as, for example, medicine, catalysis, materials science, molecular magnetism, chemical analysis, etc.[1−3] POMs have been prepared and isolated from both aqueous and nonaqueous solutions. The most common synthetic method involves acidification of alkaline aqueous solutions of simple oxoanions,[4] with the tungstate anion, WO_4^{2-}, being the main building block in the formation of polyoxotungstates. Control of the pH and temperature is also necessary. Nucleation is considered to be initiated when the WO_4^{2-} anions are protonated, $WO_3(OH)^-$, and one W−O bond is thus stretched in each tetrahedron.[4] Similarly to what happens for the molybdate anion, MoO_4^{2-}, the second $pK_{a,2}$ for WO_4^{2-} is anomalously low. Schwarzenbach et al. found in 1962 that $pK_{a,1} + pK_{a,2} = 8.1$, with both protons being lost almost simultaneously.[5] An increase of the coordination number of the metal ion upon protonation was proposed to be the origin of such low $pK_{a,2}$ values.[4] In fact, mononuclear hexacoordinated molybdenum species such as $[MoO_3(H_2O)_3]$ or $[MoO_2(OH)(H_2O)_3]^+$ have been identified at molybdate concentrations lower than 10^{-4} M and low pH values.[6] Furthermore, the rapid condensation to form POMs, which follows the protonation of WO_4^{2-} anions, may induce errors in the evaluation of pK_a's. Mononuclear and other larger cluster species in solution can also be identified using a combination of cation-exchange and electrospray-ionization mass spectrometry, as was recently shown by Cronin and co-workers for polyoxotungstates.[7] Speciation studies in vanadium inorganic and bioinorganic systems have been performed as well.[8−10] To the best of our knowledge, no theoretical studies have attempted to analyze the hydration/dehydration equilibria of molybdate or tungstate anions in solution. Messaoudi et al. have focused on the dimerization mechanisms of molybdates in aqueous solutions at very acidic conditions.[11] They have also carried out an exhaustive work about the structure and stability of VO_2^+ in aqueous

* To whom correspondence should be addressed. E-mail: antonio.rodriguezf@urv.cat (A.R.-F.), josepmaria.poblet@urv.cat (J.M.P.).

(1) Borrás-Almenar, J. J.; Coronado, E.; Müller, A.; Pope, M. T. *Polyoxometalate Molecular Science*; Kluwer Academic Publishers: Dordrecht, The Netherlands, 2003.
(2) Hill, C. L. *Chem. Rev.* **1998**, *98*, 1. Special issue on Polyoxometalates.
(3) Long, D. L.; Burkholder, E.; Cronin, L. *Chem. Soc. Rev.* **2007**, *36*, 105.
(4) Pope, M. T. *Heteropoly and Isopoly Oxometalates*; Springer-Verlag: Berlin, 1983.
(5) Schwarzenbach, G.; Geier, G.; Littler, J. *Helv. Chim. Acta* **1962**, *45*, 2601.
(6) Cruywagen, J. J.; Heyns, J. B. B. *Polyhedron* **2000**, *19*, 907.
(7) Long, D. L.; Streb, C.; Song, Y. F.; Mitchell, S.; Cronin, L. *J. Am. Chem. Soc.* **2008**, *130*, 1830.
(8) Andersson, I.; Gorzsas, A.; Kerezsi, C.; Toth, I.; Pettersson, L. *Dalton Trans.* **2005**, 3658.
(9) Baro, A. G.; Andersson, I.; Pettersson, L.; Gorzsas, A. *Dalton Trans.* **2008**, 1095.
(10) Pettersson, L.; Andersson, I.; Gorzsas, A. *Coord. Chem. Rev.* **2003**, *237*, 77.
(11) Messaoudi, S.; Furet, E.; Gautier, R.; Le Fur, E.; Pivan, J. Y. *Phys. Chem. Chem. Phys.* **2004**, *6*, 2083.

10.1021/ic8007766 CCC: $40.75
Published on Web 08/07/2008

solutions.[12] Bühl and Parrinello have also analyzed the hydration of $[VO_2(OH)_2]^-$ and $[VO_2(OH_2)_4]^+$ to elucidate the medium effects on ^{51}V NMR chemical shifts using Car−Parrinello molecular dynamics (MD) simulations.[13] With these types of atomistic simulations, it is possible to describe the bond-formation and bond-breakage processes in a self-consistent manner, treating the solute and solvent on an equal footing.[14] Unfortunately, Car−Parrinello MD are very demanding from the computational point of view, and they are typically limited to tens of solvent (water) molecules over a tens of picosecond time scale. The limited simulation time affordable by standard MD runs does not allow the observation of rare events like thermally activated chemical reactions. An alternative to this problem is given by the metadynamics method, which allows for an acceleration of the dynamics.[15−17] This method can efficiently reproduce the most probable reaction paths, clearing high barriers and providing a quite accurate picture of the free-energy profile, as demonstrated in previous applications.[18−26]

We herein study the process of hydration of hydrogentungstate anions, $WO_3(OH)^-$, at different pH conditions. Our aim is to elucidate the dependence of the coordination number of the W^{VI} ion on the pH. To achieve this objective, the inclusion of solvent effects in the computations is mandatory. First, the results of standard density functional theory (DFT) calculations in the presence of a continuous model solvent are discussed. Afterward, we go beyond the simple static approach and present the results obtained from Car−Parrinello and metadynamics simulations of a single hydrogentungstate anion with explicit water molecules and different numbers of extra protons.

Computational Details

The static calculations were carried out by using DFT methodology with the *ADF 2004* program.[27,28] The gradient-corrected functionals of Becke[29] and Perdew[30] (and Lee−Yang−Parr)[31] for the exchange and correlation energies, respectively, were used to improve the description of the electronic density provided by the local density approximation. A set of Slater-type basis functions of triple-ζ + polarization quality was employed to describe the valence electrons of all of the atoms. Frozen cores consisting of the 1s shell for O and the 1s to 4d shells for W were described by means of single Slater functions. Scalar relativistic corrections were included by means of the zeroth-order regular approximation formalism. The BP86/TZP calculations have been proven to be a very adequate methodology to study the electronic structure of POMs.[32−34] Here, we also compare the results with the Becke−Lee−Yang−Parr (BLYP) functional showing that there are no qualitative differences. All of the computed stationary points have a closed-shell electronic structure. All of the structures discussed through this work were fully optimized in the presence of a continuous model solvent by means of the conductor-like screening model (COSMO)[35,36] implemented in the ADF code.[37] To define the cavity that surrounds the molecules, we use the solvent-accessible surface method and a fine tesserae. To obtain the electron density in solution, first it is converged in the gas phase and afterward the COSMO model is turned on to include the solvent effects variationally. The ionic radii of the atoms, which define the dimensions of the cavity surrounding the molecule, are chosen to be 1.26 Å for W, 1.52 Å for O, and 1.20 Å for H. The dielectric constant is set to 78 so as to model water as the solvent.

Regarding the MD simulations, they were performed at the DFT level by means of the *CPMD* program package.[38] The description of the electronic structure is based on the expansion of the valence electronic wave functions into a plane-wave basis set, which is limited by an energy cutoff of 70 Ry. The interaction between the valence electrons and the ionic cores is treated through the pseudopotential (PP) approximation. Norm-conserving Martins−Troullier PPs are employed.[39] Nonlinear core corrections are included in the W PP.[40] We adopt the generalized gradient-corrected BLYP exchange-correlation functional.[29,31] We have checked the validity of our computational settings by computing the hydration energies for tungstic acid in the gas phase (see the Supporting Information). We have compared the results with those obtained (i) using the PP approximation and a set of Gaussian functions and (ii) the frozen-core approximation and a set of Slater orbitals. The energy differences are smaller than 2 kcal mol^{-1} (less than 10% error). In the MD simulations, the wave functions are propagated in the Car−Parrinello scheme, by integrating the equations of motion derived from the extended Car−Parrinello Lagrangian.[14] We use a time step of 0.144 fs and a fictitious electronic mass of 700 au, H atoms are substituted by D atoms. The Nosé-Hoover thermostat for the nuclear degrees of freedom was used to maintain the temperature as constant as possible around 300 K. For metadynamics calculations, a simple rescaling of the atomic velocity that keeps the temperature within an interval of 50 K around 300

(12) Sadoc, A.; Messaoudi, S.; Furet, E.; Gautier, R.; Le Fur, E.; Le Polles, L.; Pivan, J. Y. *Inorg. Chem.* **2007**, *46*, 4835.
(13) Buhl, M.; Parrinello, M. *Chem.—Eur. J.* **2001**, *7*, 4487.
(14) Car, R.; Parrinello, M. *Phys. Rev. Lett.* **1985**, *55*, 2471.
(15) Iannuzzi, M.; Laio, A.; Parrinello, M. *Phys. Rev. Lett.* **2003**, *90*, 238302.
(16) Laio, A.; Parrinello, M. *Proc. Nat. Acad. Sci. U.S.A.* **2002**, *99*, 12562.
(17) Laio, A.; Rodriguez-Fortea, A.; Gervasio, F. L.; Ceccarelli, M.; Parrinello, M. *J. Phys. Chem. B* **2005**, *109*, 6714.
(18) Biarnes, X.; Ardevol, A.; Planas, A.; Rovira, C.; Laio, A.; Parrinello, M. *J. Am. Chem. Soc.* **2007**, *129*, 10686.
(19) Blumberger, J.; Ensing, B.; Klein, M. L. *Angew. Chem., Int. Ed.* **2006**, *45*, 2893.
(20) Churakov, S. V.; Iannuzzi, M.; Parrinello, M. *J. Phys. Chem. B* **2004**, *108*, 11567.
(21) Cucinotta, C. S.; Ruini, A.; Catellani, A.; Stirling, A. *ChemPhysChem* **2006**, *7*, 1229.
(22) Ensing, B.; De Vivo, M.; Liu, Z. W.; Moore, P.; Klein, M. L. *Acc. Chem. Res.* **2006**, *39*, 73.
(23) Ensing, B.; Klein, M. L. *Proc. Nat. Acad. Sci. U.S.A.* **2005**, *102*, 6755.
(24) Rodriguez-Fortea, A.; Iannuzzi, M.; Parrinello, M. *J. Phys. Chem. B* **2006**, *110*, 3477.
(25) Rodriguez-Fortea, A.; Iannuzzi, M.; Parrinello, M. *J. Phys. Chem. C* **2007**, *111*, 2251.
(26) Stirling, A.; Iannuzzi, M.; Parrinello, M.; Molnar, F.; Bernhart, V.; Luinstra, G. A. *Organometallics* **2005**, *24*, 2533.
(27) *ADF 2004.01*; Department of Theoretical Chemistry, Vrije Universiteit: Amsterdam, The Netherlands, 2004.
(28) te Velde, G. T.; Bickelhaupt, F. M.; Baerends, E. J.; Guerra, C. F.; Van Gisbergen, S. J. A.; Snijders, J. G.; Ziegler, T. *J. Comput. Chem.* **2001**, *22*, 931.
(29) Becke, A. D. *Phys. Rev. A* **1988**, *38*, 3098.
(30) Perdew, J. P. *Phys. Rev. B* **1986**, *33*, 8822.
(31) Lee, C.; Yang, W.; Parr, R. *Phys. Rev. B* **1988**, *37*, 785.
(32) Fernandez, J. A.; Lopez, X.; Bo, C.; de Graaf, C.; Baerends, E. J.; Poblet, J. M. *J. Am. Chem. Soc.* **2007**, *129*, 12244.
(33) Lopez, X.; Weinstock, I. A.; Bo, C.; Sarasa, J. P.; Poblet, J. M. *Inorg. Chem.* **2006**, *45*, 6467.
(34) Poblet, J. M.; Lopez, X.; Bo, C. *Chem. Soc. Rev.* **2003**, *32*, 297.
(35) Andzelm, J.; Kolmel, C.; Klamt, A. *J. Chem. Phys.* **1995**, *103*, 9312.
(36) Klamt, A.; Schuurmann, G. *J. Chem. Soc., Perkin Trans. 2* **1993**, 799.
(37) Pye, C. C.; Ziegler, T. *Theor. Chem. Acc.* **1999**, *101*, 396.
(38) *CPMD*; IBM Corp.: Armonk, NY, 1990−2006; MPI für Festkörperforschung: Stuttgart, Germany, 1997−2001.
(39) Troullier, N.; Martins, J. L. *Phys. Rev. B* **1991**, *43*, 1993.
(40) Louie, S. G.; Froyen, S.; Cohen, M. L. *Phys. Rev. B* **1982**, *26*, 1738.

Scheme 1. Species with a Five-Coordinated W^{VI} Ion Obtained after the Incorporation of a Single Water Molecule to $WO_3(OH)^-$, $WO_2(OH)_2$, and $WO(OH)_3^+$[a]

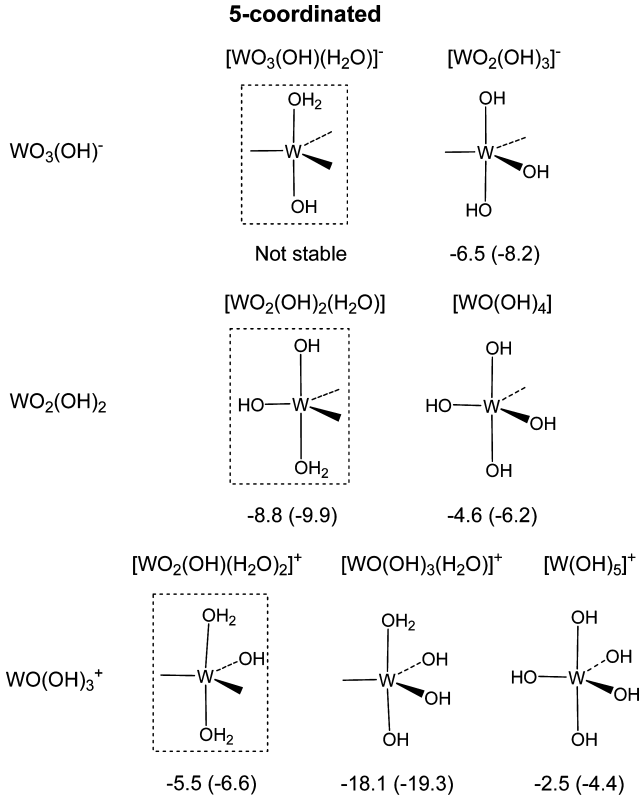

[a] The hydration energies, $A + H_2O \rightarrow A{\cdot}H_2O$ [$A = WO_3(OH)^-$, $WO_2(OH)_2$, and $WO(OH)_3^+$], in kcal mol^{-1}, computed with the BP86 and BLYP (in parentheses) functionals are also shown. The structural isomers considered in Car−Parrinello MD simulations are highlighted.

K is used. The cell box that contains one $WO_3(OH)^-$ [or $WO_2(OH)_2$ or $WO_2(OH)(H_2O)^+$] and 29 water molecules ($a = b = c = 9.959$ Å) is repeated periodically in space by the standard periodic boundary conditions. Initial geometries for the simulations were created by substituting 3 water molecules from an equilibrated classical MD simulation of liquid water (32 water molecules in a box of the same size) with a hydrogentungstate anion. Initialization runs of at least 0.5 ps followed by at least 3 ps of equilibration are performed prior to the MD production runs.

Results and Discussion

The reaction energies for the incorporation of a water molecule to $WO_3(OH)^-$, $WO_2(OH)_2$, and $WO(OH)_3^+$, i.e., for the formation of five-coordinated $[WO_3(OH)(H_2O)]^-$, $[WO_2(OH)_2(H_2O)]$, and $[WO(OH)_3(H_2O)]^+$ complexes, respectively, computed at standard DFT/COSMO with the BP86 and BLYP (in parentheses) functionals are collated in Scheme 1. The reaction energies for the structural isomers that would be formed after intramolecular proton transfer in the aforesaid complexes are also shown in Scheme 1. Only the value for the most stable geometric isomer (*cis*, *trans*, *mer*, and *fac* for the relative positions of the oxo, hydroxo, and aqua ligands) for each structural isomer is shown. Similarly, the reaction energies for the formation of the six-coordinated complexes after the incorporation of 2 water molecules are collated in Scheme 2.

Scheme 2. Species with a Six-Coordinated W^{VI} Ion Obtained after the Incorporation of Two Water Molecules to $WO_3(OH)^-$, $WO_2(OH)_2$, and $WO(OH)_3^+$[a]

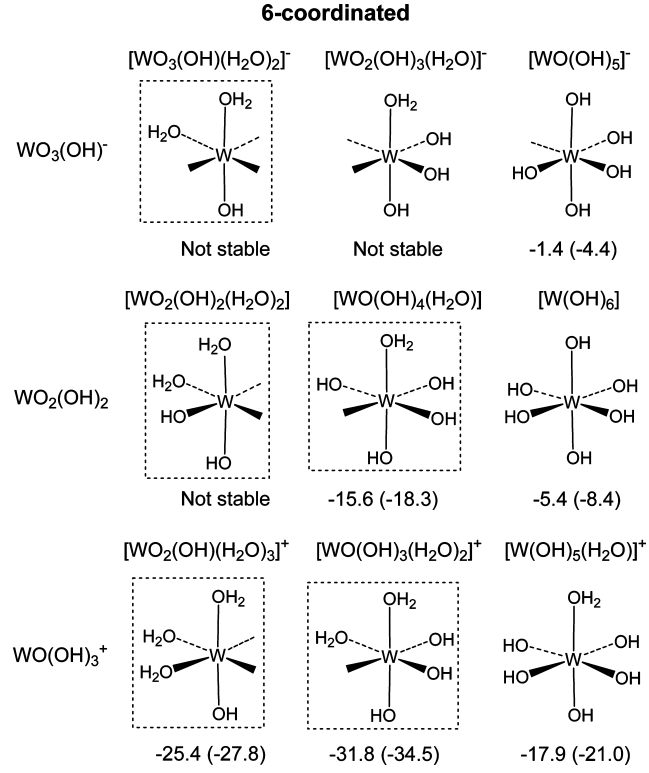

[a] The hydration energies, $A + 2H_2O \rightarrow A{\cdot}(H_2O)_2$ [$A = WO_3(OH)^-$, $WO_2(OH)_2$, and $WO(OH)_3^+$), in kcal mol^{-1}, computed with the BP86 and BLYP (in parentheses) functionals are also shown. The structural isomers considered in Car−Parrinello MD simulations are highlighted.

For the case of the hydrogentungstate anion, $WO_3(OH)^-$, the complexes with aqua ligands directly attached to the W^{VI} ion are not stable, regardless of the coordination of this ion. However, the complexes with hydroxo ligands are somewhat more stable than reactants for the two coordination numbers five and six. Interestingly, the reaction is somewhat more exothermic when the coordination number of the W^{VI} ion is five, regardless of the functional used. For the neutral acid, $WO_2(OH)_2$, reaction energies are more exothermic than those for the hydrogentungstate anion and coordination six is somewhat more favored than five. It is important to note that the six-coordinated complex with two aqua ligands is not stable at this level of computation. Finally, for the most acidic species, $WO(OH)_3^+$, reaction energies are fairly exothermic for both coordination numbers five and six, especially for the latter. In this case, all of the complexes that contain aqua ligands are stable. The hydration energies obtained with the BLYP functional are slightly more exothermic than those found with BP86, but the qualitative trends are the same.

Therefore, the results obtained when performing static DFT calculations at the BP86/COSMO (or BLYP/COSMO) level indicate as a general and *qualitative* trend that higher coordination numbers for the W^{VI} ion are favored when the concentration of protons is increased, i.e., the pH is lowered, in aqueous solutions of tungstate anions. As the number of protons in the complex increases, the W^{VI} ion becomes more

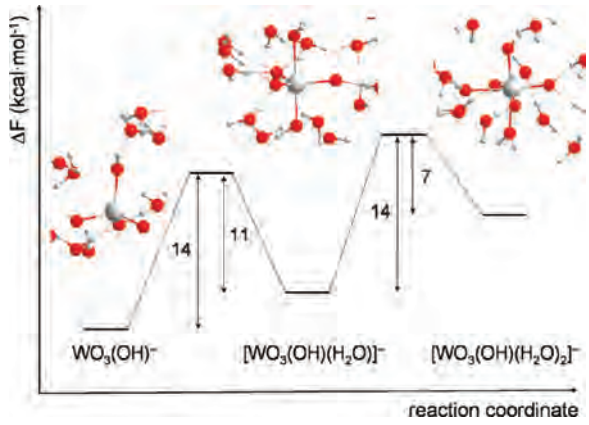

Figure 1. Free-energy profile (in kcal mol^{-1}) corresponding to the hydration/dehydration equilibria of a hydrogentungstate anion.

electrophilic and it is more effectively bound to nucleophilic aqua ligands. A *quantitative* analysis requires the computation of free energies in solution with the inclusion of explicit water molecules.[12,41,42]

From now on, we will describe the results obtained including explicit solvent molecules carried out by means of Car−Parrinello MD and metadynamics simulations. We have analyzed the free-energy changes that are a consequence of the incorporation of water molecules to the coordination sphere of W^{VI} ions at different pH conditions. Because of the large number of structural isomers involved in these equilibria (see Schemes 1 and 2), we have only considered those isomers that are highlighted in the schemes.

To obtain the free-energy profile for the hydration/dehydration equilibria of a hydrogentugstate anion (eqs 1 and 2),

$$WO_3(OH)^- + H_2O \rightleftarrows [WO_3(OH)(H_2O)]^- \quad (1)$$

$$[WO_3(OH)(H_2O)]^- + H_2O \rightleftarrows [WO_3(OH)(H_2O)_2]^- \quad (2)$$

we have performed several metadynamics simulations.[43] As shown in Figure 1, the four-coordinated tetrahedral $WO_3(OH)^-$ anion is somewhat more stable (3 kcal mol^{-1}) than the five-coordinated trigonal-bipyramidal structure. The free-energy barriers for the interconversion of the four- to five-coordinated species and vice versa are far from being negligible (14 and 11 kcal mol^{-1}, respectively).

Concerning the six-coordinated $[WO_3(OH)(H_2O)_2]^-$ anion, it is even more unstable than the five-coordinated $[WO_3(OH)(H_2O)]^-$ anion with a free energy that is 10 kcal mol^{-1} higher than the lowest-energy tetrahedral species. Moreover, the barrier that has to be overcome to obtain it is as large as 17 kcal mol^{-1}. Assuming that the Helmholtz free energy is close to the Gibbs energy, the approximate equilibrium constants for processes 1 and 2 are predicted to be log $K_1 = -2.2$ and log $K_2 = -5.1$. So, the hydrogentungstate anion in a water solution keeps the tetrahedral coordination most of the time. The six-coordinated species with two extra aqua ligands will be observed very rarely, but the probability of finding the five-coordinated complex is not so low.

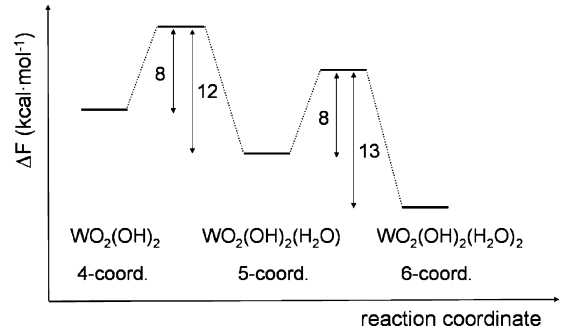

Figure 2. Free-energy profile (in kcal mol^{-1}) corresponding to the hydration/dehydration equilibria of tungstic acid.

To analyze the effect that acidification of the solution has on the incorporation of water molecules to the coordination sphere of the W^{VI} ion, we have studied the following equilibria (eqs 3 and 4):[44]

$$WO_2(OH)_2 + H_2O \rightleftarrows [WO_2(OH)_2(H_2O)] \quad (3)$$

$$[WO_2(OH)_2(H_2O)] + H_2O \rightleftarrows [WO_2(OH)_2(H_2O)_2] \quad (4)$$

Tungstic acid is the predominant species in solution when the pH is slightly lower than the p$K_{a,1}$. The computed free-energy profile relative to $WO_2(OH)_2$ is depicted in Figure 2. Now, the relative stability of the different species is changed. The most stable compound is that with the six-coordinated W^{VI} ion, $[WO_2(OH)_2(H_2O)_2]$, which is 5 and 9 kcal mol^{-1} more stable than the five- and four-coordinated species, respectively. Moreover, the barrier for the formation of the six-coordinated species (8 kcal mol^{-1}) is much lower than that in the case of the hydrogentungstate anion (17 kcal mol^{-1}). The approximate equilibrium constants for processes 3 and 4 are predicted to be log $K_3 = 2.91$ and log $K_4 = 3.64$, respectively.

Once the tungstate is diprotonated, the W^{VI} ion of the tungstic acid is more electrophilic than that in the case of the hydrogentungstate anion. As a result, the W^{VI} ion is more easily attacked by the nucleophilic water molecules, thus decreasing the barrier for the formation of the aqua complexes.

Therefore, a decrease of the pH of the aqueous solution involves an *expansion* of the coordination sphere of the W^{VI}

(41) Buhl, M.; Diss, R.; Wipff, G. *J. Am. Chem. Soc.* **2005**, *127*, 13506.
(42) Buhl, M.; Kabrede, H.; Diss, R.; Wipff, G. *J. Am. Chem. Soc.* **2006**, *128*, 6357.

(43) In all of the metadynamics runs that we have performed, we have chosen as the collective variable the distance between the W^{VI} ion and the O atom of a nearby water molecule. We have done one simulation for each of the following processes: (i) $WO_3(OH)^- + H_2O \rightarrow [WO_3(OH)(H_2O)]^-$. The parameters used in this run are $k = 0.2$ au and $M = 10$ amu. The height of the hills (W) is 0.31 kcal mol^{-1}, their perpendicular width ($\Delta s^{\perp}$) 0.1, and the deposition rate (Δt) 0.0144 ps. The estimated error (ϵ) in the computation of the free energy is 1 kcal mol^{-1}. The total simulation time (t_{total}) was 9 ps. (ii) $[WO_3(OH)(H_2O)]^- \rightarrow WO_3(OH)^- + H_2O$. $k = 0.2$ au, M = 10 amu, $W = 0.19$ kcal mol^{-1}, $\Delta s^{\perp} = 0.1$ au, $\Delta t = 0.0144$ ps, $\epsilon = 1$ kcal mol^{-1}, and $t_{total} = 19$ ps. (iii) $[WO_3(OH)(H_2O)]^- + H_2O \rightarrow [WO_3(OH)(H_2O)_2]^-$. Same parameters as those for (i), except $t_{total} = 11.5$ ps. (iv) $[WO_3(OH)(H_2O)_2]^- \rightarrow [WO_3(OH)(H_2O)]^- + H_2O$. Same parameters as those for (ii), except $t_{total} = 5$ ps.

(44) Different metadynamics runs were performed. One for each of the following processes: (i) $WO_2(OH)_2 + H_2O \rightarrow [WO_2(OH)_2(H_2O)]$. Same parameters as those for the previous metadynamics, except $W = 0.19$ kcal mol^{-1} and $t_{total} = 25$ ps. (ii) $[WO_2(OH)_2(H_2O)] \rightarrow WO_2(OH)_2 + H_2O$. Same parameters as those for (i), except $t_{total} = 17$ ps. (iii) $[WO_2(OH)_2(H_2O)] + H_2O \rightarrow [WO_2(OH)_2(H_2O)_2]$. Same parameters as those for (i), except $t_{total} = 9$ ps. (iv) $[WO_2(OH)_2(H_2O)_2] \rightarrow [WO_2(OH)_2(H_2O)] + H_2O$. Same parameters as those for (i), except $W = 0.25$ kcal mol^{-1} and $t_{total} = 6$ ps.

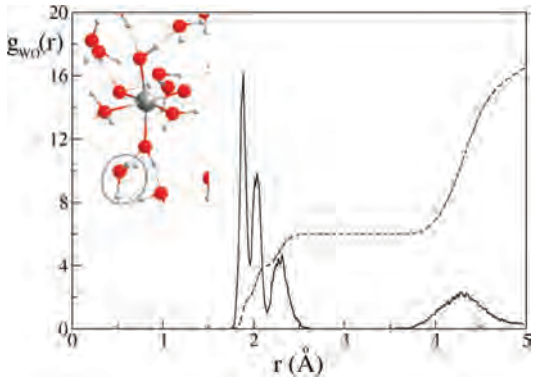

Figure 3. W−O radial distribution function (solid line) and its integration (broken line) computed for the 15 ps MD simulation starting from $[WO_2(OH)(H_2O)_3]^+$. The geometry of the six-coordinated species along with the nearest water molecules that solvate it is shown at the left top corner. The formed hydronium ion is highlighted.

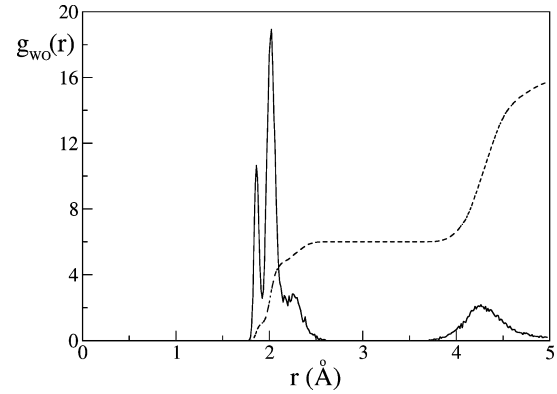

Figure 4. W−O radial distribution function (solid line) and its integration (broken line) computed for the 13 ps MD simulation starting from $[WO(OH)_3(H_2O)_2]^+$.

ion, as was supposed from the experimental results. It is also important to note that the most stable complex $[WO_2(OH)_2(H_2O)_2]$ calculated when doing Car−Parrinello metadynamics simulations is predicted to not be stable within the continuous COSMO model.

Finally, we have also examined the behavior of tungstic acid solutions at high acidic conditions, i.e., when the pH is considerably lower than $pK_{a,1}$, looking at the fate of the six-coordinated structural isomers $[WO_2(OH)(H_2O)_3]^+$ and $[WO(OH)_3(H_2O)_2]^+$ (see Scheme 2). During the metadynamics[45] for $[WO_2(OH)(H_2O)_3]^+$, one proton is released from a water molecule coordinated to the W^{VI} ion, yielding the neutral tungstic acid $[WO_2(OH)_2(H_2O)_2]$ and a hydronium ion in the solution. The released proton recombines several times with the tungstic acid, recovering the former $[WO_2(OH)(H_2O)_3]^+$ cation. The free-energy barrier from the six- to five-coordinated cation is 13 kcal mol^{-1}, in good agreement with the results obtained for the tungstic acid. Because we have not accelerated the deprotonation/protonation equilibrium with any collective variable, we conclude that the barriers for proton transfers in such a system are low. Indeed, we have performed a standard Car−Parrinello MD simulation for 15 ps on the six-coordinated $[WO_2(OH)(H_2O)_3]^+$ cation, and we have observed almost from the beginning the aforementioned proton transfers and the formation of tungstic acid $[WO_2(OH)_2(H_2O)_2]$ in solution. The W−O radial distribution function and its integration, which yields the W−O coordination number,[13] are displayed in Figure 3.

The sharp spike below 2 Å that integrates two O atoms can be attributed to the oxo ligands. The spike at around 2 Å that integrates two more O atoms corresponds to the hydroxo ligands. Finally, the third spike between 2 and 2.5 Å, which integrates the other two O atoms, is due to the aqua ligands coordinated to the W^{VI} ion. At distances between 2.5 and 3.7 Å, the W−O coordination number shows a plateau associated with the presence of six O atoms in the coordination sphere of the W^{VI} ion. A shallow maximum appears between 4 and 4.5 Å, which is ascribed to the first solvation sphere. This solvation sphere can be estimated to contain, on average, 10 water molecules. It is important to note here that some water molecules of the first solvation sphere are exchanged reversibly with those of the remaining solvent during the simulation.

A similar phenomenon occurs in the case of the structural isomer $[WO(OH)_3(H_2O)_2]^+$: at the beginning of a standard Car−Parrinello MD simulation, one proton from an aqua ligand is released, giving again an isomer of tungstic acid $[WO(OH)_4(H_2O)]$ and a hydronium ion in the solution. The simulation was extended up to 13 ps. During the first 1 ps, the hydronium ion recombines with tungstic acid, recovering the former $[WO(OH)_3(H_2O)_2]^+$ cation. Afterward, once the hydronium is released again, the isomer of tungstic acid $[WO(OH)_4(H_2O)]$ remains for around 7 ps. Then, the protonated cation $[WO(OH)_3(H_2O)_2]^+$ is recovered again and lasts up to the end of the simulation. The W−O radial distribution function and its integration are displayed in Figure 4.

Two well-separated spikes between 1.8 and 2.1 Å, which correspond to the oxo and hydroxo ligands, are now distinguished. The third spike, which is centered at 2.3 Å and corresponds to the aqua ligand, is not now so well defined. The three spikes integrate up to six O atoms, but the distribution pattern of ligands around W^{VI} is different. Now there is only one oxo ligand. Regarding the distribution of hydroxo and aqua ligands around W^{VI}, the ratio of their averaged coordination numbers is approximately 3.5:1.5, a consequence of the existence of both neutral tungstic acid $[WO(OH)_4(H_2O)]$ and the protonated cation $[WO(OH)_3(H_2O)_2]^+$ for similar periods during the simulation. The shallow maximum between 4 and 4.5 Å associated with the first solvation shell is also present. From the results of our simulations, we infer that at high acidic conditions (i) proton transfers between protonated tungstic acid and the solvent molecules are likely events and (ii) tungstic acid and its structural isomers have a higher probability of being found as neutral than as protonated. For even lower pH values, which would have to be simulated with a larger number of protons in the unit cell, the protonated form of tungstic acid will become the most likely species.

(45) Same parameters as those for the previous metadynamics, except W = 0.19 kcal mol^{-1} and t_{total} = 5 ps.

Conclusions

We have used standard DFT techniques as well as Car−Parrinello MD simulations with the explicit inclusion of solvent molecules to study the hydration/dehydration equilibria of a hydrogentungstate anion, tungstic acid, and protonated tungstic acid. On the basis of reaction energies and free-energy profiles, we have confirmed that an increase of the acidity of the solution, i.e., a decrease of the pH, involves an expansion of the coordination sphere of the W^{VI} ion in good agreement with experimental results. Furthermore, we have found that, at the conditions of our simulations, protonated tungstic acid has preference to be deprotonated. Much higher acidic conditions would have to be simulated to find protonated tungstic acid as the most likely species. Regarding continuous solvation models, we should pay attention when using them because they are not able to predict as stable the lowest-energy hydrated tungstic acid found when doing Car−Parrinello metadynamics. Continuous solvation models have been shown to yield a good description of geometries and orbital energies of polyoxoanions in solution.[46] However, some problems had already appeared when explicit aqua ligands were introduced in combination with continuous models of solvation.[47] So, to include the effect of the first solvation shell on the free-energy barriers, the incorporation of explicit solvent molecules in the computations is mandatory. Our study provides a quantitative picture of the hydration equilibria of a hydrogentungstate anions in acidic solutions, which is fundamental for further understanding of the nucleation processes that yield POMs.

Acknowledgment. This work was supported by the Spanish Ministry of Science and Technology [Project No. CTQ2005-06909-C02-01/BQU and the Ramón y Cajal Program (A.R.-F.)] and by the DURSI of the Generalitat de Catalunya (Grant 2005SGR-00104).

Supporting Information Available: Cartesian coordinates for the optimized structures shown in Schemes 1 and 2 and a table with details concerning the validation of the PP. This material is available free of charge via the Internet at http://pubs.acs.org.

IC8007766

(46) Lopez, X.; Fernandez, J. A.; Romo, S.; Paul, J. F.; Kazansky, L.; Poblet, J. M. *J. Comput. Chem.* **2004**, *25*, 1542.
(47) Romo, S.; Fernandez, J. A.; Maestre, J. M.; Keita, B.; Nadjo, L.; de Graaf, C.; Poblet, J. M. *Inorg. Chem.* **2007**, *46*, 4022.